DEVELOPMENT OF AN ELASTIC BASE WITH TWO DEGREES OF FREEDOM FOR VIV STUDIES

Cesar Monzu Freire, cesar.freire@poli.usp.br
Ivan Korkischko , ivan.korkischko@poli.usp.br
NDF, Department of Mechanical Engineering, POLI, University of São Paulo, CEP 05508-900, São Paulo, SP, Brazil

Julio R. Meneghini, jmeneg@usp.br
NDF, Department of Mechanical Engineering, POLI, University of São Paulo, CEP 05508-900, São Paulo, SP, Brazil

Abstract. *Vortex shedding occurs when a cylinder is immersed in a fluid current. In some conditions, the alternate shedding of vortices can make the cylinder vibrate. This phenomenon is called Vortex-Induced Vibrations (VIV). VIV is very important in some particular engineering areas, such as the offshore industry. A great amount of papers analyzed VIV in one degree of freedom, in which the cylinder is free to oscillate in the transverse direction to the flow. The influence of the motion in-line with the flow remains not entirely known. Having as target to increase knowledge about the VIV phenomenon with two degrees of freedom, an elastic base was developed and installed in the water channel facility at the Fluid & Dynamics Research Group (NDF). The design of this base and the first results are shown in this paper. Two different designs are analyzed. The first one uses flexible cables and the other one a rigid beam. To articulate the rigid beam a link ball and a Cardan joint were tested. The implemented base uses the Cardan joint and has low values of mass and structural damping.*

Keywords: *vortex shedding, vortex-induced vibrations, structural damping , experimental fluid dynamics*

1. INTRODUCTION

This paper will present the main project parameters of an elastic base. It is very important to design such equipment with versatility. In VIV studies a circular cylinder is immersed in an uniform current flow. As the velocity of the flow changes, the cylinder motion may change. Several papers analyzed the response of the cylinder when it could vibrate in one degree of freedom, transverse to the flow. The elastic base presented in this work gives the cylinder the possibility to oscillate in two degrees of freedom.

The cylinder is mounted in the elastic base. The mechanical parameters of the base defines how the cylinder will respond to the current in which is immersed. The mass, natural frequency and structural damping are the most important parameters of the base. To choose the materials to be used in this equipment, all these parameters were analyzed.

Jauvtis and Williamson (2003) studied VIV with two degrees of freedom. Their elastic base design used four cables to suspend an structure where the cylinder was mounted. Their conclusion was that the second degree of freedom did not affect the response obtained in one degree of freedom, so all the previous data obtained for VIV studies with just one degree of freedom were useful to understand the whole phenomenon. In this experimental study the mass coefficient m^* is close to 7. More about VIV studies are available in Williamson and Govardhan (2004).

The elastic base developed in the present work has the aim to reproduce the same kind of work developed by Jauvtis and Williamson (2003). Different conditions of mass coefficient, Reynolds number and external appendix on the cylinder will be tested. This paper focus on design of the elastic base. VIV results obtained with the developed equipment will be presented in further papers.

2. MATHEMATICAL MODEL

Several designs could be used to allow the cylinder to vibrate in two degrees of freedom. Each one has its own advantages and disadvantages. Two designs were analyzed to be used in the elastic base.

A very simple design is to use a pendulum with cables. This design has the advantage of having a very low oscillating m, consisting mostly in the mass of the cylinder and some other auxiliar parts. The structural damping ζ has also a low value, because there are few points of contact between different parts, avoiding friction. The problem of this solution consists that to work appropriately the base needs high values of mass ratio ($m^* >> 1$). The advantage of having low oscillating mass m becomes a disadvantage. The cables cannot resist to compression loads, so the base weight must be greater then the thrust force caused by the water. If $m^* < 1$ the cylinder will float.

Even if $m^* \approx 1$ the cylinder may rotate. To avoid these difficulties, m^* should be high. Jauvtis and Williamson (2003) used a similar elastic base. In that work, experiments were made using different values of m^*, starting with $m^* = 5$ and finishing at $m^* = 25$.

Another way to avoid the cylinder to float or to rotate is to use rigid cables or a beam. If the mass of this rigid element

Table 1. Symbols

Cylinder diameter	D	
Natural frequency in water	f_N	
Gravity acceleration	g	
Mass ratio	m^*	$\frac{m}{\pi\, L_m\, D^2\, \rho_w}$
Structural damping	ζ	$\frac{c}{2\sqrt{k\, m}}$
Normalized velocity	V_r	$\frac{U_\infty}{f_N\, D}$
Normalized tip amplitude	A^*	A/D

represents a great part of the global mass of the base and depending on how the cylinder is mounted on it, it is important to consider the pendulum effect.

Occasionally, the pendulum effect could be used as the only source of restitution force. The natural frequency of a concentrated mass m oscillating in a L length pendulum is given by eq.(1) and the natural frequency of the same mass, oscillating with a spring is given by eq.(2).

$$f_{n-pendulum} = \frac{1}{2\pi}\sqrt{\frac{g}{L}} \tag{1}$$

$$f_{n-spring} = \frac{1}{2\pi}\sqrt{\frac{k}{m}} \tag{2}$$

Figures 1 and 2 show the ideas presented above. The design with rigid bean was selected because it allowed a light base, with small values of m^*. The motion of each base has its own characteristics. The "four cables" base has a translation movement and the articulated base has a rotational movement. In both designs the pendular and the elastic spring effects are important for the base mechanical behavior.

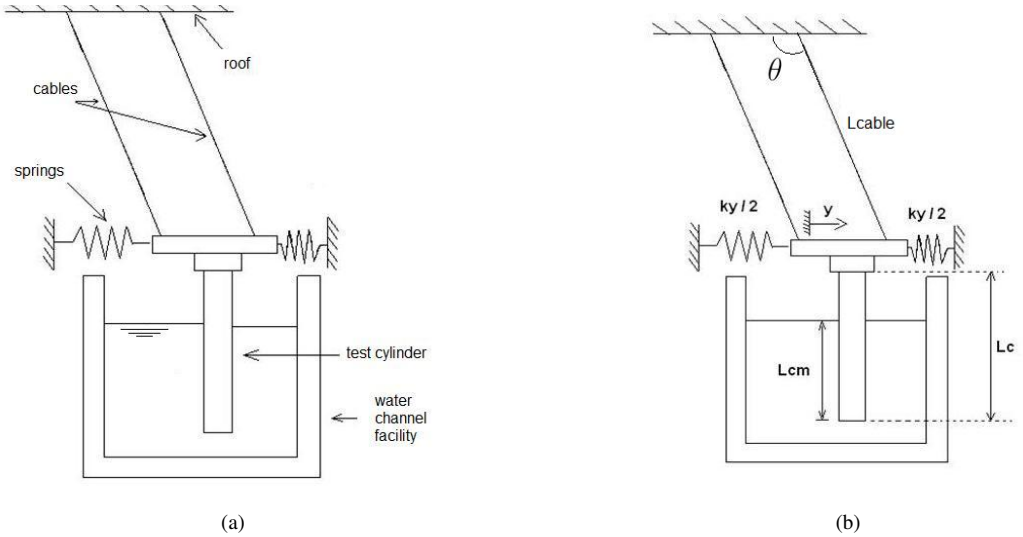

(a) (b)

Figure 1. Four cables design base

The eq.(3) and eq.(4) shows the estimative of the natural frequency of each design.

$$f_N^{4\,cables} = \frac{1}{2\,\pi}\sqrt{\frac{k_y}{m_t + m_w} + \frac{(m^* - C_w)}{(m^* + C_w)}\,\frac{g}{L_{cabo}}} \tag{3}$$

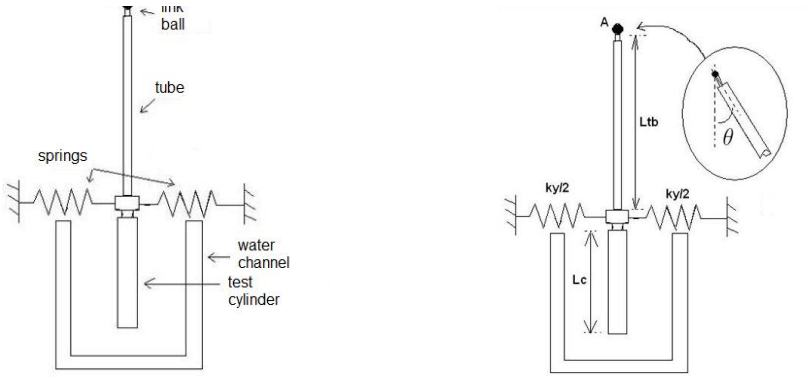

(a) (b)

Figure 2. Articulated design base

$$f_N^{articulated} = \frac{1}{2\,\pi}\sqrt{\frac{g}{(J+J_w)}\left[m_{tb}\,\frac{L_{tb}}{2} + m_{cab}\,L_{tb} + (m_c - m_d)\,\left(L_{tb} + \frac{L_c}{2}\right)\right] + \frac{k_y\,L_{tb}^2}{(J+J_w)}} \tag{4}$$

In eq.(4), J and J_w represents the moment of inertia of the whole elastic base and the moment of inertia of the displaced water.

As it was mentioned before, the "four cables" design requires high values of m^*. The design selected was the articulated base. The articulation was first made using a link ball, presented in figure 3(a). With this kind of link the elastic base had a high value damping coefficient ($\zeta = 0.06$).

One of the aims of the elastic base was to have a low ζ value. An idea to reduce this coefficient is to avoid friction between parts, so a Cardan joint using ball bearings, as shown in figure 3(b), was designed and implemented. This modification caused the reduction of the damping coefficient to a very low value $\zeta = 0.002$.

(a) (b)

Figure 3. (a) Link ball (b) Cardan joint

3. COMPONENTS AND MATERIALS

The elastic base was made using three principal materials. Most of the parts were made of aluminium, while some of the parts were made of acrylic. The beam/tube used as a pendulum is made of titanium.

There are some basic functions in the pendular elastic base. These functions can be itemized by:

- Fixation in the laboratory's roof
- Articulation
- Connections
- Pendulum
- End gap tuning
- Laser targets

- Spring connection

The fixation in the roof is made by the part shown in the figure 4(a). The articulation, as mentioned above, is made by the Cardan joint. The higher connection part is shown in the figure 4(b). This part connects the titanium tube used as a pendulum to the Cardan joint.

Figures 4(d) and 4(c) illustrates the parts responsible to fix the test cylinder in the titanium tube. The part shown in the picture 4(c) can be positioned in a way to minimize the gap existente between the end of the test cylinder and the water channel ground. It is very importante to control the gap because in this region the tip vortex can introduce some tridimensionalities in the flow.

(a) (b) (c) (d)

Figure 4. Aluminium parts of the elastic base

Figures 5(a), 5(b) and 5(c) illustrates the acrylic parts of the elastic base. The first one shows the target where the laser sensor are pointed. The second one is used to fix the conector shown in the figure 4(c). This ring is outside the titanium tube and uses a screw that pass through a hole in the tube to fix the conector. The third image shows the spring conector. As it is possible to see in the figure, the conector has four groups of three holes. Each group will receive one or two springs. For one spring the middle hole is used, and for two springs, the first and the third are used.

(a) (b) (c)

Figure 5. Acrylic parts of the elastic base

4. DETERMINING THE SPRINGS LENGTH

The reduced velocity V_r is defined as a function of the natural frequency of the elastic base where the cylinder is mounted. In bases with just one degree of freedom, it is easy to measure and control this frequency, because it is given by the frequency of a spring-mass system, see eq.(2).

In the developed base, the second degree of freedom creates a non-linearity. To simplify the problem the pendulum effect influence is ignored. Considering that the base consists in four springs arranged like the figure 6, the equivalent spring coefficient in one of the principal directions x and y is given by eq.(5).

$$k_{y-eq} = \frac{F_{1y} - F_{2y} - F_{3y} - F_{4y}}{y} \tag{5}$$

In the equation below F_{iy} represents the F_i component in the direction y. These forces are given in the next equations.

$$F_{1y} = k_y \frac{L_{my} - y}{\sqrt{(L_{my} - y)^2 + x^2}} \left(\sqrt{(L_{my} - y)^2 + x^2} - L_{my} \right) \tag{6}$$

$$F_{2y} = k_x \frac{y}{\sqrt{(L_{mx} - x)^2 + y^2}} \left(\sqrt{(L_{mx} - x)^2 + y^2} - L_{mx} \right) \tag{7}$$

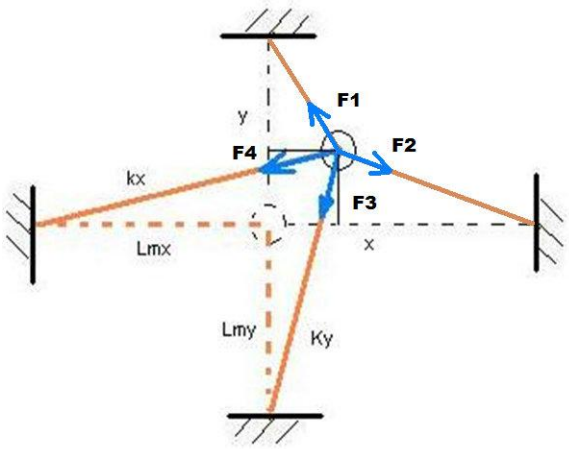

Figure 6. Spring error analysis scheme

$$F_{3y} = k_y \frac{L_{my} + y}{\sqrt{(L_{my} - y)^2 + x^2}} \left(\sqrt{(L_{my} + y)^2 + x^2} - L_{my} \right) \tag{8}$$

$$F_{4y} = k_x \frac{y}{\sqrt{(L_{mx} + x)^2 + y^2}} \left(\sqrt{(L_{mx} + x)^2 + y^2} - L_{mx} \right) \tag{9}$$

It is very importante to avoid the non-linearity presented in the equations shown above. As we can see in these equations, if the initial lengths were infinity, the forces caused in the direction y by the springs positioned in the direction x vanish. In this case each direction would move independently one from the other. If the size of the initial lengths were small, by the same order of the displacements x and y, then the forces caused in one direction by the springs in the other direction would have the same order. That nonlinearity could make the natural frequency vary during the test, for each position (x, y).

Plotting the error of the spring coefficient, defined by the eq.(10), it is possible to determine one acceptable value for L_{mx} and L_{my}.

$$Error_{spring} = \frac{k_y - (k_{y-eq})}{k_{y-eq}} \, 100\% \tag{10}$$

Figure 7 shows the error caused by the nonlinearity. Considering acceptable a 2% error, the springs must have at least $40cm$ length.

5. EXPERIMENTAL ARRANGEMENTS

The elastic base developed in this paper is installed at the NDF water channel facility, shown in the figure 8(b). This channel can operate at good quality and well controlled flow at velocities up to $0.7m/s$ with average turbulency intensity lower than 2%, and the follow dimensions: height: $h_c = 0.9m$, width $w_c = 0.7m$ and length $l_c = 7.5m$. More information about the water channel are available in Ássi (2005). The position measurement instrument is a laser optic sensor LEUZE (ODSL 8/V4 model). The force measurements instrument is a BSL (PME1 model) load cell.

In the experiments, the flow velocity varied from zero to $0.3m/s$. The velocity is varied, and after 120 seconds, a 180-second measurement signal is obtained. The two minutes between each measurement are very important to avoid transient effects caused by the variation of the velocity of the channel U_∞. In the experiments U_∞ is kept constant.

The same experiment must be realized twice. First the velocity is increased and thereafter the velocity is decreased. The objetive of these two experiments is to investigate the hysteresis effect existent in the VIV phenomenon.

The load cells are mounted on the fixed end of the springs, as shown in the figure 8(a). The force measured this way is not the hydrodynamic forces F_y^w directly. The force applied on the load cell is the spring restoration term $k_y\, y$. The hydrodynamic forces can be obtained by eq.(11).

$$m\,\ddot{y} + c\,\dot{y} + k_y\, y = F_y^w \tag{11}$$

In eq.(11) the damping term $c\,\dot{y}$ can be ignored because the value of the damping coefficient $\zeta = c/2\sqrt{k\,m}$ is very low, $\zeta = 0.002$. The inertia term $m\,\ddot{y}$, can be measured with an accelerometer, or by numerical differentiation of the data

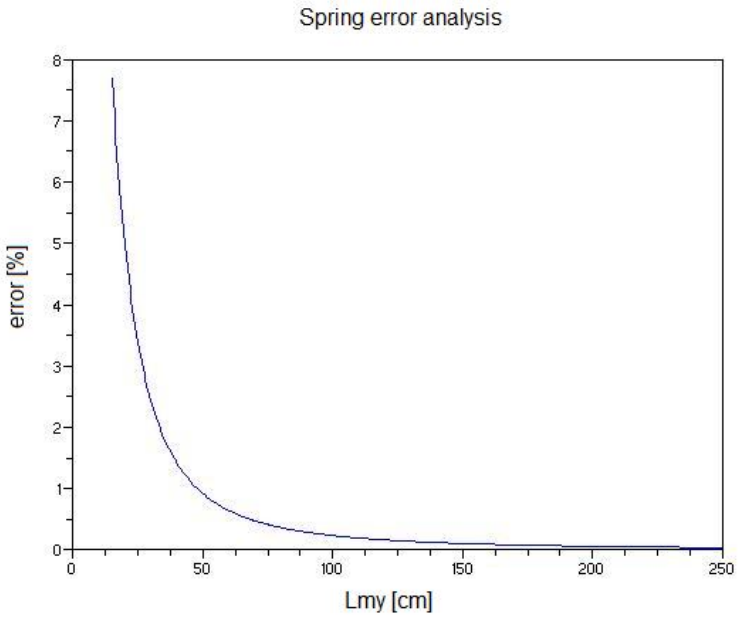

Figure 7. Spring error evaluation

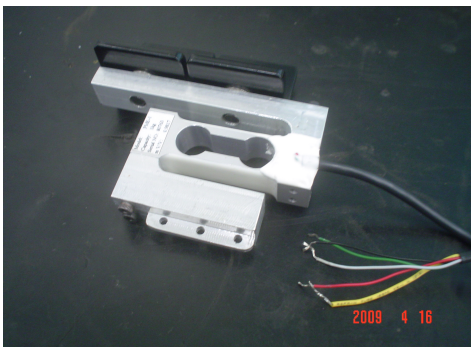

(a)

(b)

Figure 8. (a) Force measurement sensor (b) NDF water channel facility

obtained with the optic position sensor. Numerically, the relation between a second derivative of a signal $\frac{d^2f}{dx^2}|_i$ and the signal $f(i)$ can be given by the eq.(12).

$$\frac{d^2f}{dx^2}|_i = \frac{f(i+1) - 2\,f(i) + f(i-1)}{(\Delta x)^2} \tag{12}$$

6. RESULTS AND DISCUSSION

Several experiments were made using the elastic base developed in this paper. In this section the results of the free-decay test is presented.

A small displacement in the base is applied and then the base oscillates without external forces. Two kinds of free-decay tests can be used. In one of them there is no cylinder immersed. This test is called air free-decay. In the other one, the cylinder is mounted in the elastic base, and it is called water free-decay.

In the air free-decay, the cylinder mass is added in the elastic base, so the total mass remains the same. Without the cylinder, there is no water influence, so the damping measured is only the structural damping of the elastic base.

The water-free-decay is not used to define the damping coefficient of the system because the hydrodynamic damping is very high, when compared to the structural damping. This test is important to measure the natural frequency of the system in water. This value is very important, as it is used to calculate the reduced velocity V_r.

To obtain the damping coefficient, the maximum value of each oscillation is compared, as shown in eq.(13).

$$\frac{2\,\pi\,\zeta}{\sqrt{1-\zeta^2}} = \frac{1}{n}\,\ln\left(\frac{Y_i}{Y_{i+n}}\right) \tag{13}$$

For low values of ζ, eq.(13), can be simplified to eq.(14).

$$\zeta = \frac{1}{2\,\pi\,n}\,\ln\left(\frac{Y_i}{Y_{i+n}}\right) \tag{14}$$

In the equations above, n is the number os oscillations used in the analysis. Y_i is the value of the maximum displacement in the $i-th$ oscillation, and Y_{i+n} is the maximum displacement n oscillations after. More about the free-decay method can be found in Beards (1996). The natural frequency is obtained by taking the dominant frequency of a Fourier transform of the displacement signal.

Figures 9(a) and 9(b) show the free-decay results for the elastic base using the link ball and the Cardan joint. It can be seen the strong influence of the damp coefficient in the response of the elastic base. This result shows that the replacement of the link ball by the Cardan joint decreased enormously the structural damping coefficient.

7. CONCLUSION

The elastic base developed has low mass ($m^*_{min} = 1.46$) and very low structural damping coefficient ($\zeta \approx 0.002$). It allows experiments with different values of mass ratio and natural frequency. The base can be modified to operate in just one degree of freedom. The maximum reduced velocity obtained with this base is close to 40. Figure 10 shows the elastic base developed. This equipment is ready to be used in VIV studies with one or two degrees of freedom.

8. ACKNOWLEDGEMENTS

The authors wish to acknowledge the financial support of FAPESP, Petrobras and FINEP and the technical work related to the parts manufacture carried out by Douglas Silva. The authors also acknowledge the useful comments and suggestions given by Guilherme Rosa Franzini.

9. REFERENCES

Beards, C. F., 1996, "Structural vibrations: analysis and dampin", Arnold.

Jauvtis, N., Williamson, C. H. K., 2003, "Vortex-induced vibration of a cylinder with two degrees of freedom", Journal of Fluids and Structures 17, 1035–1042.

Ássi, G. R. S., 2005, "Estudo experimental do efeito de interferência no escoamento ao redor de cilindros alinhados", Master's thesis, EPUSP, São Paulo.

Williamson, C. H. K., Govardhan, R., 2004, "Vortex-induced vibrations", Ann. Rev. Fluid Mech. 36, 413–455.

10. Responsibility notice

The authors are the only responsibles for the printed material included in this paper.

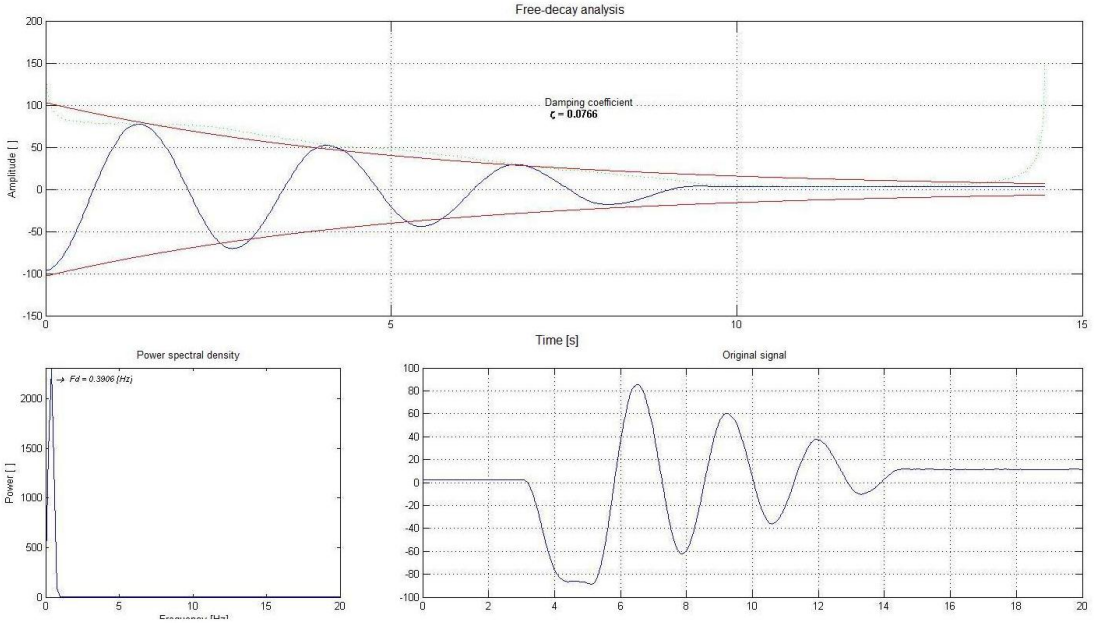

(a)

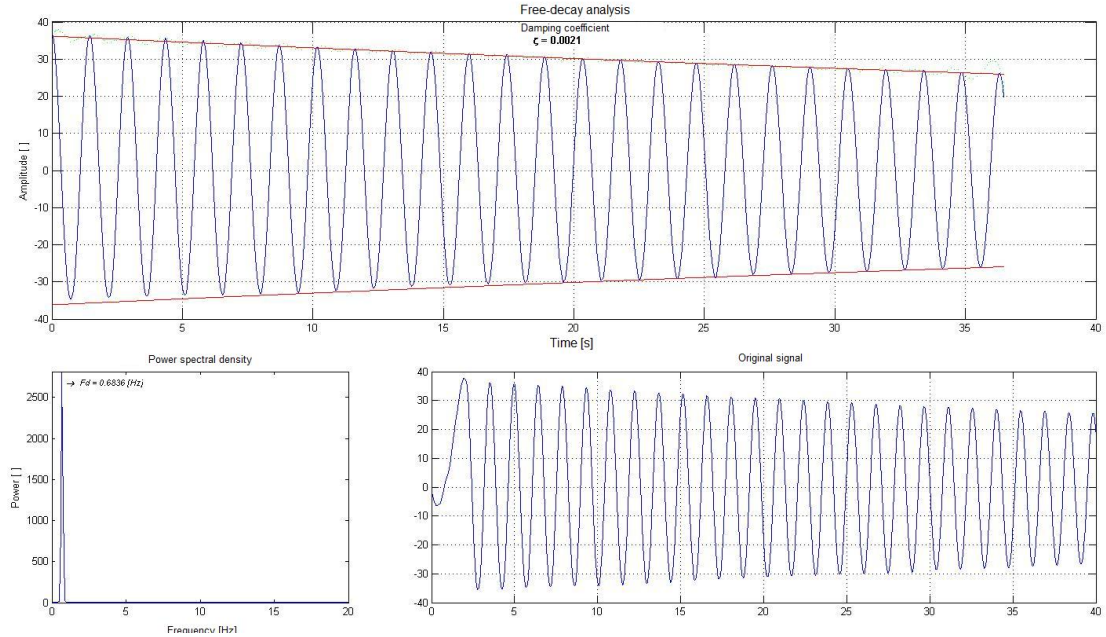

(b)

Figure 9. Free-decay result using (a) link ball (b) Cardan joint

Figure 10. Elastic base developed